

Nonlinear Seismic Assessment of Historical Masonry Karaz Bridge Under Different Ground Motion Records

Ömer Faruk NEMUTLU^{1,2*}, İhsan GÜZEL^{1,2}, Bilal BALUN^{2,3}, Mitat ÖZTÜRK⁴, Ali SARI⁵

¹Department of Civil Engineering, Bingöl University

²Bingöl University Centre for Energy, Environment and Natural Disasters

³Department of Architecture, Bingöl University

⁴Department of Civil Engineering, Osmaniye Korkutata University

⁵Faculty of Civil Engineering, İstanbul Technical University

(ORCID: [0000-0001-7841-3911](https://orcid.org/0000-0001-7841-3911)) (ORCID: [0000-0002-0746-070X](https://orcid.org/0000-0002-0746-070X)) (ORCID: [0000-0003-0906-4484](https://orcid.org/0000-0003-0906-4484))

(ORCID: [0000-0003-4685-7088](https://orcid.org/0000-0003-4685-7088)) (ORCID: [0000-0002-6888-1276](https://orcid.org/0000-0002-6888-1276))



Keywords: Finite element method, Masonry bridges, Nonlinear dynamic analysis, Failure, Earthquake behaviour.

Abstract

The most significant artifacts that transfer the cultural heritage of past civilizations to the present are historical structures. Historical bridges are of great importance in terms of transportation, trade and architecture from past to present. Some of these structures have been destroyed by natural disasters or have suffered significant structural damage. Especially earthquakes cause damage to these structures. In this study, the earthquake behavior of the Historical Karaz Bridge was investigated. The structural elements of the bridge and the materials connecting the bearing elements were evaluated together with the macro modeling approach. For this purpose, a 3D finite element model of the bridge was generated and its seismic behavior under different ground motion records was investigated by nonlinear analysis. Analyzes were carried out using the ground motion records of Bingöl, Elazığ, Erzincan, Van and Gölcük, and the results were evaluated mutually. In the analysis results, the dynamic behavior of the bridge was evaluated over the distribution of displacements and stresses and the earthquake behavior was investigated.

1. Introduction

Bridges have been an important part of transportation routes throughout history. Historical bridges, on the other hand, establish a link between the past and the present, apart from their intended use in their time. It is important to protect these bridges as they reflect their period socially and culturally. Therefore, historical bridges should be preserved and passed on to future generations. It should be kept as far away from environmental influences as possible for durability and sustainability. Climatic conditions, fires, wars and all the situations they are exposed to reduce the useful life of historic bridges. Otherwise, vehicle loads, human loads and earthquake loads cause historical bridges to decrease in strength, to be damaged and to collapse completely as seen in some

historical bridges. Historical bridges are one of the historical structures that are accepted as cultural heritage. These structures, which have a history of hundreds of years, should be preserved in the best way and transferred to the future. Earthquakes are one of the most important external factors that cause damage to historical structures. In order for these structures to suffer the least damage from earthquakes and to protect their structural integrity, seismic behavior should be determined, and necessary precautions should be taken accordingly. Most of the historical bridges were built as masonry stone walls. These bridges consist of foundation, arch, side wall and filling material, and the superstructure forming the carrier part was built using stone and binding material [1–3].

*Corresponding author: ofnemutlu@bingol.edu.tr

Received: 01.01.2022, Accepted: 01.06.2022

Vibrations occur during earthquakes and these vibrations cause historic bridges to reach significant levels of damage [4,5]. By design, historical structures are important. Bridges built on different dates in the past were generally built as arches. Arch form is the general structural carrier system of historical bridges [6]. The arch-shaped structure is a suitable design system for passing wide openings due to its positive behavior to pressure forces due to its geometric form. Stone or brick was used as the main building material in the construction of the arches due to their resistance to high pressures [2,3,7]. The importance of historical bridges in terms of engineering as well as social life has encouraged researchers to work in this field. Studies that investigating the seismic behavior of historical masonry bridges with linear and nonlinear finite element models are available in the literature [1, 2, 8-28]. After analyzing 3 historical palaces with the finite element models, Valente ve Milani [18] studied the crack development, earthquake behavior with nonlinear dynamic analysis, and made a general assessment of damage and collapse. Karaton et al. examined the earthquake behavior of historical Malabadi bridge, which was built in the 12th century and located in the east of Turkey, for different earthquake levels [25]. As a result of the study, D1, D2 and D3 are from the lowest to the highest ground motion level, no significant damage occurred at the ground motion levels D1 and D2; it was observed that the historic bridge suffered substantial damage at the D3 ground motion level. Güllü [2] created a finite element model for the Historic Cendere Bridge, using earthquake scenarios suitable for the seismicity of the region where the bridge is located, and performed linear analyzes in the time domain. As a result of the analyzes made, it has been observed that the vulnerability of the historical bridge in possible during an earthquake is high. Özmen ve Sayın [6], created a finite element model for the historical Dutpınar Bridge and investigated its dynamic behavior using the records of the 2003 Bingöl earthquake, one of the most destructive earthquakes that occurred in the region. At the end of the study, the maximum and minimum displacement values for the critical structural members were examined. Bayraktar et al. [24] determined analytical and experimental vibration parameters of a historical two-span bridge built in the 19th century and located in northern Turkey. Comparing the natural frequency, mode shapes, and damping rates for analytical and experimental results, the authors observed slight differences. Pela et al. [17] investigated the earthquake behavior of two different historical bridges by using nonlinear static analysis methods for

different modern standards. As a result, they concluded that the nodes at the top of the bridges are an important point in determining seismic capacity. Işık et al. [19] studied the historical Ahlat Emir Bayındır bridge and made observational and analytical seismic evaluations in this study. After the field studies, they explained how similar structures would be evaluated.

In this study, the seismic response of the historical Karaz (Öznü) bridge was modeled and analyzed using the ABAQUS program using different earthquake records reflecting the seismicity of the region. As a result of the study, the stressed areas on the bridge were determined for different earthquake records and the displacements occurred during the earthquake period were obtained.

2. Historical Karaz (Öznü) Bridge

The historical Karaz bridge is located 5 km northeast of the Karaz District (Village), just to the right of the International Erzurum Airport and the ring road. Coordinates of bridge are 39.967-41.147. It was built in the period to provide transportation on the Karasu River. The building does not have an inscription, but it is estimated that it was built in the 16th century when Erzurum joined the Ottoman lands and development activities were concentrated.

The bridge was repaired by the General Directorate of Highways between 1980-1984. In the meantime, the old stones were replaced, and the periphery of the flood splitter was supported with triangular reinforced concrete elements. Then, in 2017, it was restored by the 12th Regional Directorate of Highways. The historical Karaz bridge is 135 m long and 6.6 m wide in the east-west direction and has eight arches. Seven of them were built with low pointed arches where the water flows fast and hard, and the eighth was built with smaller, round arches at the far end. The spans and heights of the bridges are not equal to each other, some of them are arranged with low pointed arches and some with narrower pointed arches. On the upstream side, which is the incoming direction of the water, there are triangular-bottom floods covered with a half-pyramidal cone and six round-bottomed heels in the downstream direction of the water. The bridge reaches the middle point with a slight inclination towards the middle from both ends and the height of the bridge is 7.70 meters from the ground, and it is limited by stone railings on both sides. The materials used in the bridge were smooth cut stone on the facades and rubble stone with plenty of mortar in between. The historical Karaz bridge still continues to provide transportation services especially between the surrounding villages. The

current view and location of the Historical Masonry Karaz bridge are given in Figure 1.



Figure 1. Historical Karaz bridge views and location of Karaz bridge

3. Material and Method

The Historical Masonry Karaz bridge is located in the northeast of Karlıova district of Bingöl is located of the intersection of the North Anatolian Fault (NAF) and East Anatolian Fault (EAF) one of Turkey's active fault zones. Therefore, Karaz bridge, which is within the boundaries of Erzurum province, has a significant earthquake risk potential.

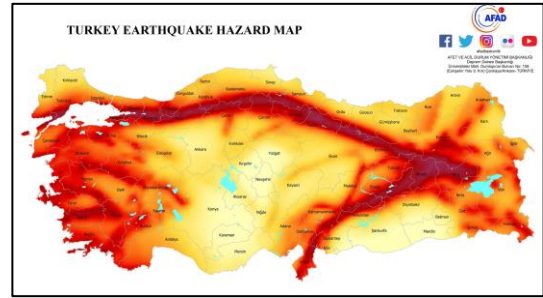
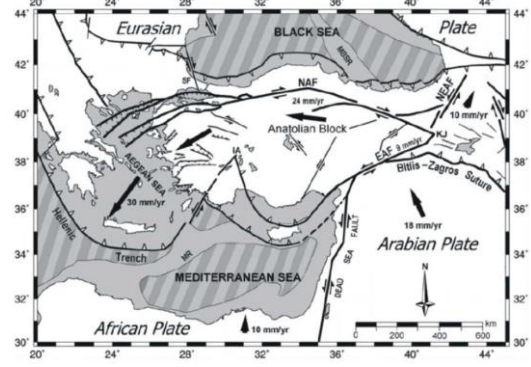


Figure 2. Turkey's active fault map [28] and Turkey earthquake hazard map [29]

The Turkey's active fault map is given in Figure 2. By using Turkey Earthquake Hazard Map, the necessary earthquake parameters are generated for the coordinates of the bridge [29]. Since there is no clear information about the ground properties of the Karasu river and its surroundings, the ground class was accepted as ZC (the middle of the soil classification made according to the TEC 2018) according to the classification used in Turkish Earthquake Code 2018 [30]. Turkey Earthquake Hazard Map overview is given in Figure 2 and the data taken from the earthquake hazard map are given in Table 1. The information about the earthquakes used in the analyzes are given in Table 2, the acceleration spectrum used for scaling the earthquake records in Figure 3, and the ground motion records (acceleration-time) and scaled records of 5 earthquakes considered within the scope of the study are given in Figure 4 and 5.

Table 1. Data from the earthquake hazard map

Earthquake Ground Motion Level	DD-2
Local Soil Class	ZC
Latitude-Longitude	39.967991-41.14791
S_s	0.717
S_1	0.214
PGA	0.3
PGV	18.985

Analyzes were completed using the acceleration records of the Gölcük, Bingöl, Van,

Erzincan and Elazığ earthquakes (only in the z direction) and these analyzes were named as A1, A2, A3, A4 and A5, respectively. First, the horizontal elastic response spectrum was created from the Turkey earthquake hazard map by using the location of the bridge [29]. The reason for choosing these ground motion records is to take into account the earthquakes that occurred in the region where the bridge is located and the Gölcük earthquake that occurred in Turkey, which is frequently used in the literature.

The scaled earthquake records given in Figure 5 were used in the analysis. The earthquake records

were scaled by the SeismoMatch [31] program using the horizontal elastic response spectrum in Fig. 9, and the minimum period and maximum period were 0.2T and 1.5T (ASCE7), respectively [32]. In order to shorten the analysis time, specific parts of the records used were taken into account. The first 10 seconds for A1, 10 seconds between 20-30 seconds for A2, 40 seconds between 20-60 seconds for A3, first 30 seconds for A4 and 30-70 seconds for A5.

Table 2. Selected ground motion records

Code	Earthquake	Record Station	Mw	Epicentral Distance (km)	Shear Wave Velocity (m/sn)
A1	Gölcük (1999)	5401	7.2	35.87	412
A2	Bingöl (2003)	1201	6.4	11.80	529
A3	Van (2011)	6503	6.7	42.24	N/A
A4	Erzincan (1992)	2402	6.1	12.82	455
A5	Elazığ (2020)	2308	6.8	23.81	450

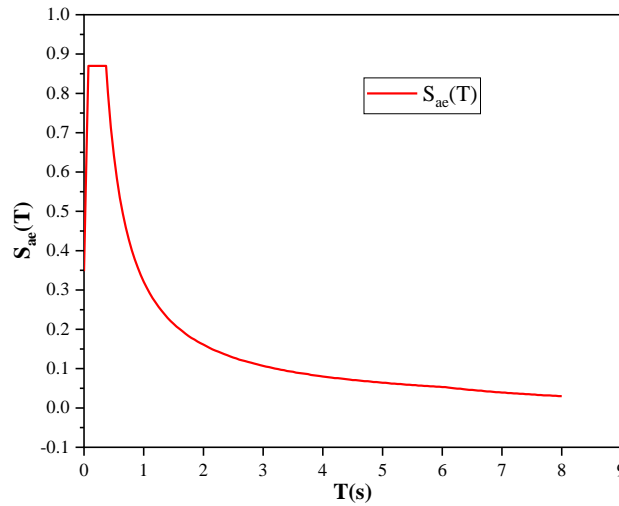
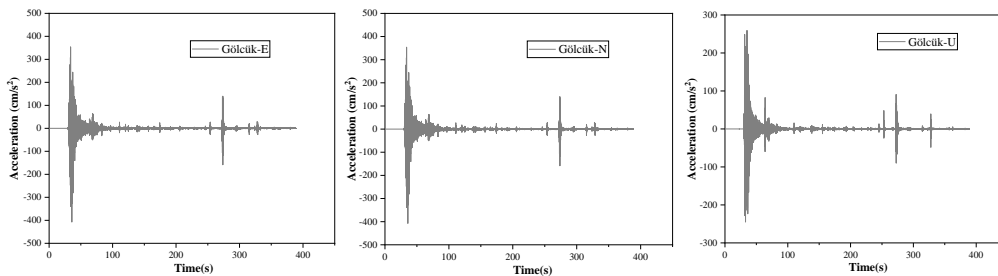


Figure 3. Horizontal Elastic Acceleration Spectrum



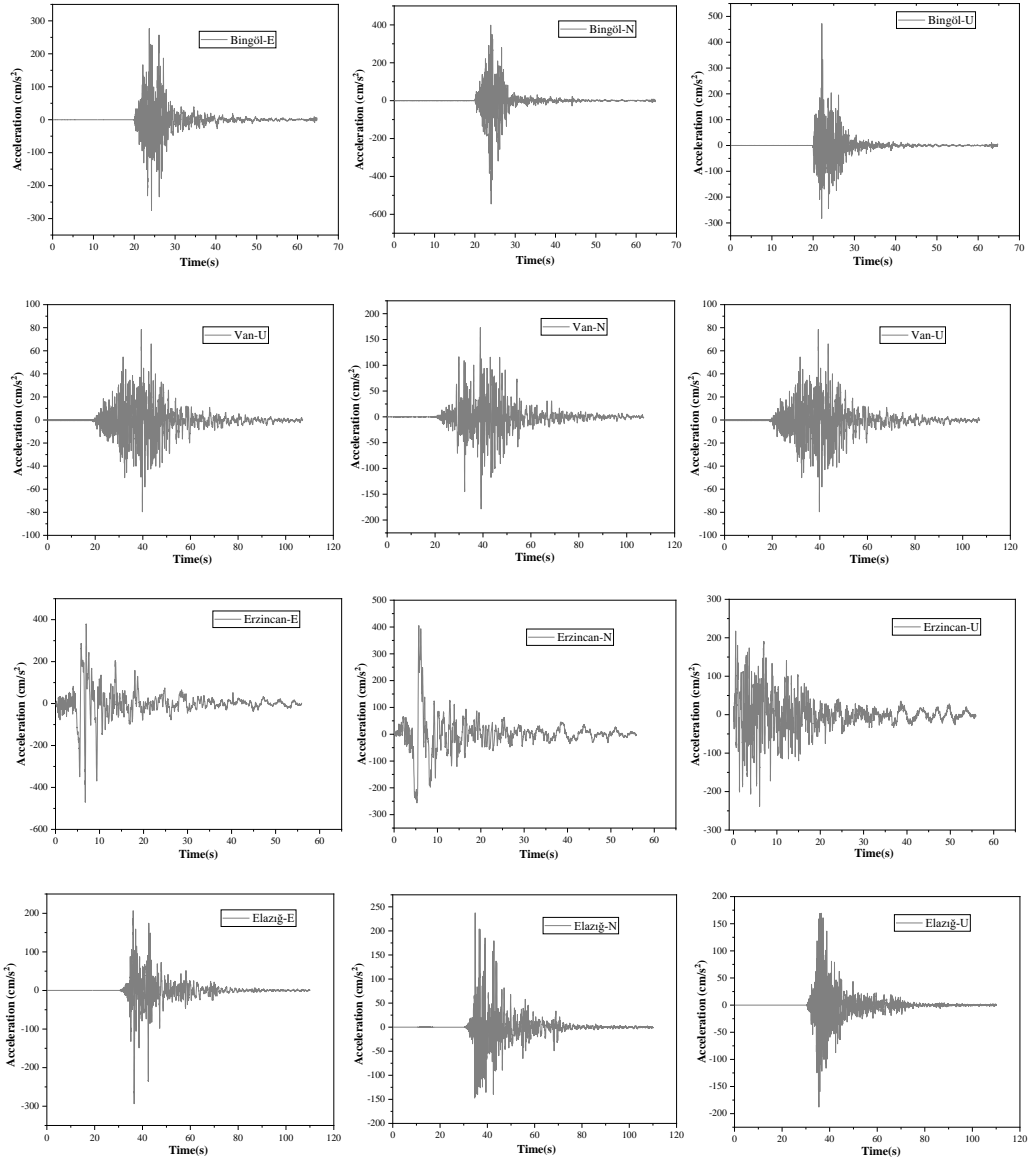


Figure 4. Earthquake acceleration records

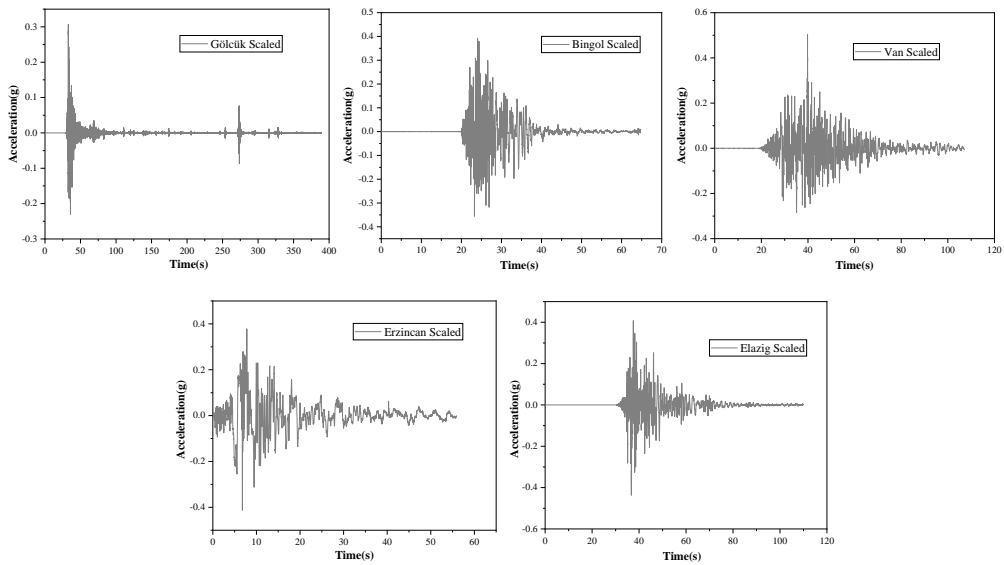


Figure 5. Scaled earthquake records

4. Methodology

In the scope of the study, 3 dimensional 10-node tetrahedral C3D10 finite elements are used as a finite element model. The C3D10 element is a general-purpose tetrahedral element (4 integration points). Shape functions can be found in Figure 6. Node numbering follows the rule in Figure 6. Element behavior is very good and is a good general-purpose element, but the C3D20R element is available in the literature where it gives better results for the same number of degrees of freedom. The C3D10 element may be particularly preferred due to the availability of fully automatic tetrahedral networks [33].

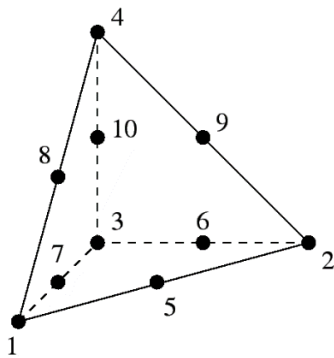


Figure 6. 3-dimensional 10 nodes tetrahedral C3D10 finite element [25]

Whether the finite element network is sufficient for analysis should be considered in the analysis. If the element network is "good enough", it can be said that the analysis results are also acceptable, assuming all other inputs of the model are correct. Finite element density is an important metric used to check the accuracy of the analysis (element type and shape also affect the accuracy of the analysis). Assuming that there is no region of singularity in the model, a high-density network structure will produce results with high accuracy. However, large amounts of computer memory and long runtimes will be required if the network of elements in the model is very dense. This disadvantage is frequently encountered especially for multiple iteration conditions specific to nonlinear and transient analysis. One of the ways to evaluate the quality of a finite element network is to compare the results with test data or theoretical values. Unfortunately, test data and theoretical results are often not available in the early stages of the study. Therefore, other tools are

required to assess network quality. The most basic and most accurate method for evaluating the quality of the mesh is to tighten the mesh with smaller elements until the maximum stress convergence at a given location is achieved (mesh convergence). Within the scope of this study, mesh size to be used was determined by making mesh optimization. By comparing the number of elements and frequencies belonging to the 1st mode, the mesh size to be used in the study was selected as 600 mm. In Table 3, mesh size, number of elements and frequencies of the first mode are given. In Figure 7, mesh convergence graph is given.

Table 3. Optimization of meshes

Mesh size (mm)	Number of elements	1.mode frequency (Hz)
400	232506	19.28
500	113770	19.29
600	79704	19.31
750	36789	19.37
1000	18788	19.42
1250	10255	19.52
1500	8025	19.58
1750	6066	19.66
2000	4587	19.71

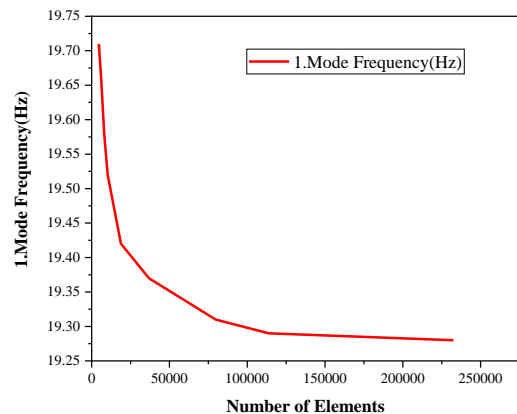


Figure 7. Mesh convergence graph

4.1. Numerical Modeling

Three methods are commonly used in modeling masonry structures. Modeling techniques are given in Figure 8 [6]. In detailed micro modeling, the masonry unit, and the material properties of the mortar i.e., elasticity modulus, Poisson ratio and unit volume weights are evaluated separately. This modeling technique is

one of the best techniques for modeling the behavior of masonry walls. Thus, damage and collapse mechanisms can be simulated properly. However, this method makes the analysis of the entire structure difficult and prolongs the solution time. This modeling technique is particularly suitable for small structures or solving parts of the structure. In simplified micro modeling, the size of the masonry units is expanded by half the thickness of the mortar layer, neglecting the mortar layer. Masonry units are separated from each other by interfacial lines. It is accepted that the cracks that will occur in the system will occur at these interface lines. Macro modeling, on the other hand, is an equivalent material model that accepts the building element as composite and reflects the common feature of these materials, without making any distinction between stone and brick blocks and mortar [34]. This method is generally preferred because it significantly reduces the computer solution time in modeling large systems [26]. The three-dimensional solid model of the Historical Masonry Karaz bridge to be used in this study, prepared in the ABAQUS program, is given in Figure 9 and its geometric properties are given in Figure 10.

Concrete Damage Plasticity (CDP) model is adopted to simulate the nonlinear behavior of the wall. Although originally developed to describe the nonlinear behavior of concrete [35,36], the use of such a model for masonry is widely accepted in the literature after proper adaptation of the main parameters. The CDP model is a damage model based on continuous plasticity, allowing different tensile and compressive strength as in the wall, with different damage parameters in stress and compression. The CDP model considers the effect of closing preformed cracks under cyclic loading conditions, resulting in compression stiffness recovery.

Masonry Bridge material specified as green part is modeled with linear and nonlinear parameters and Base material specified as white part is modeled with linear parameters only. The general analysis procedure and accepted material properties in this study were based on the studies of Valente and Milani [18] and Güllü [2]. In Table 4, material properties for analysis and in Table 5, damage values and stress strain values for the CDP model are given.

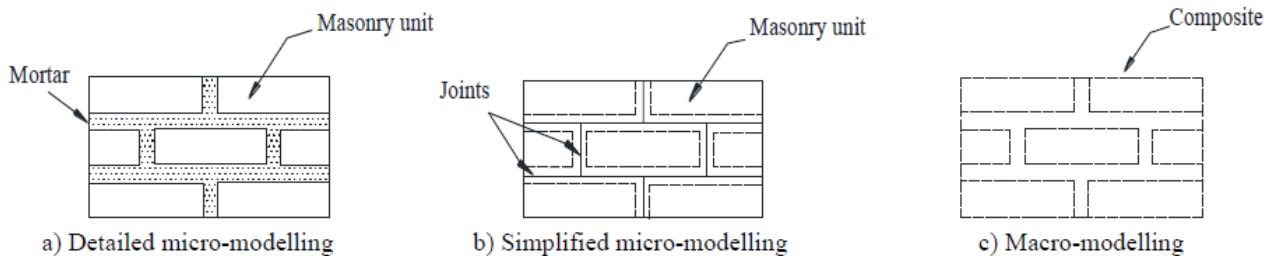


Figure 8. Modeling Approaches [6]

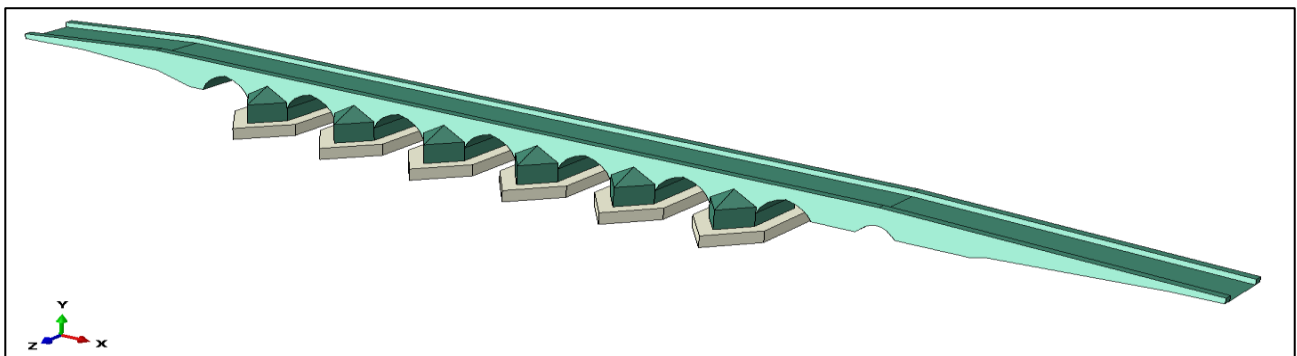


Figure 9. Solid Model of the Karaz bridge

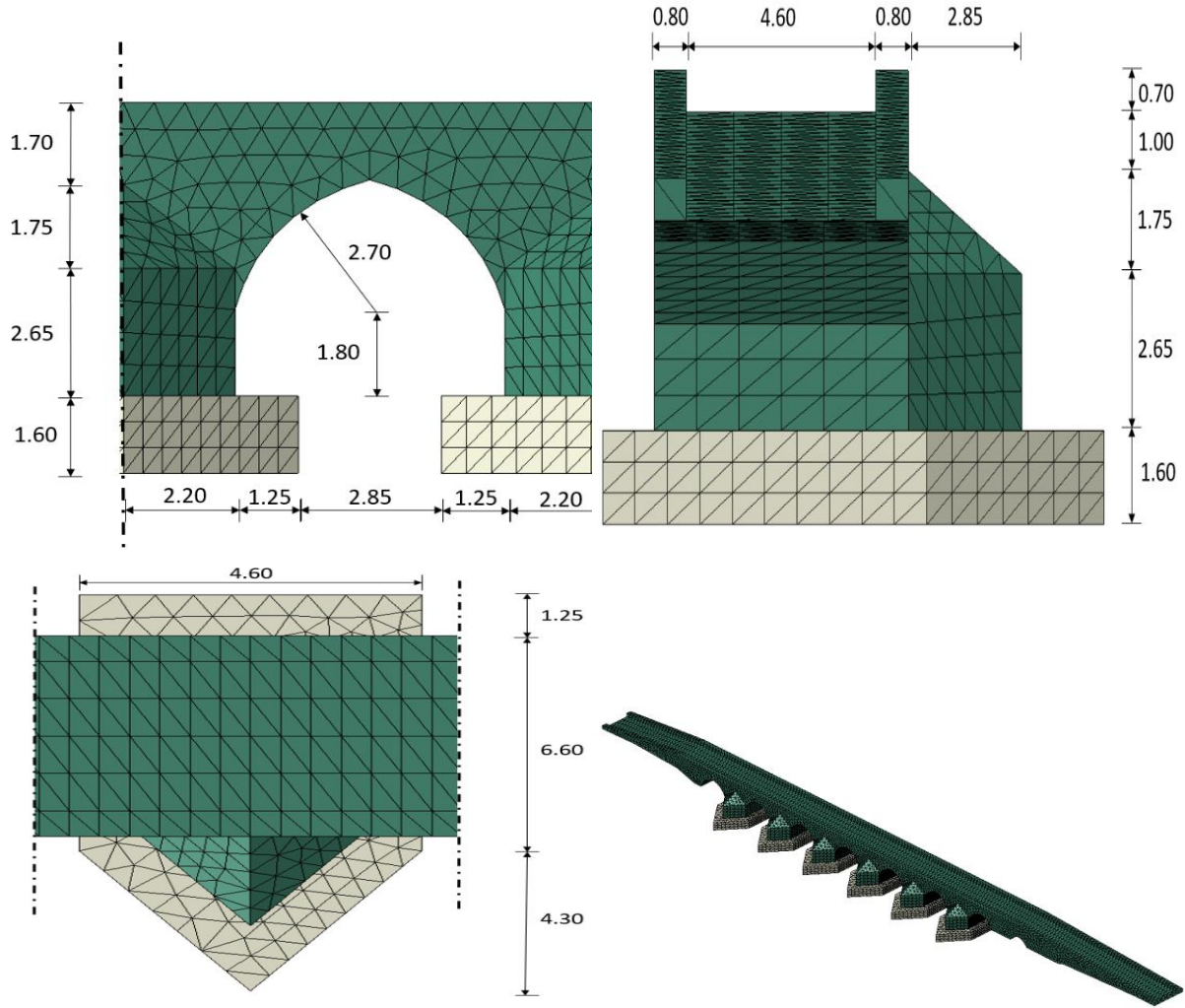


Figure 10. Geometric Properties of the Karaz bridge

Table 4. Linear Material Properties [2,18]

	E (Young Modulus) MPa	ν (Poisson Ratio)	Mass Density (t/mm^3)
Masonry Bridge	3500	0.25	2.20E-09
Base	5000	0.3	2.40E-09

Table 5. Uniaxial stress–strain values and scalar damage values utilized in the CDP model for masonry [18]

Non-linear Material Properties (mansory brigde)										
Concrete Damaged Plasticity					Tensile Behavior				Compressive Behavior (type strain)	
Dil Angle	E_{cc}	f_b/f_c	K	Vis	Yield Stress	Cracking Strain	Damage	Crack strain	Yield Stress	Inelastic Strain
					0.15	0	0	0	1.9	0
10	0.1	1.16	0.666	0.001	0.075	0.00025	0.95	0.00121	2.4	0.0051
					0.018	0.00057			0.96	0.0102
					0.009	0.00121			0.48	0.0307

5. Results

Since the stresses (compression, tensile) caused by its own weight (constant load) are lower than the material strength, no damage is expected in the stone arch bridge under constant load. The unfavorable earthquake motion affecting the bridge has been determined by calculating the stresses due to earthquake-induced loads separately for the maximum (tensile), minimum (pressure) and maximum acceleration of the stress envelope. It can be said that this tensile stress obtained is compatible with the tensile strength/compressive strength ratios (1/20-1/10) proposed by Pela [17] for masonry structures and can be used as a control in the assessment of damage potential. However, it would be appropriate to stay on the safer side due to factors arising from the loading situation (dead, earthquake, and dead+earthquake), analysis type (linear) and lack of experimental data. Therefore, as mentioned before, in this study, the damage potential was evaluated by

assuming the tensile strength / compressive strength ratio as 1/20 or 5%. Therefore, it has been predicted that structural strength may decrease, and damage may occur at values greater than 1/20 (> 1 MPa) of tensile stress under earthquake effect. After the analysis, free vibration modes and corresponding frequency values are given in Figure 11 for the first 4 modes.

When the period values of free vibration modes calculated by modal analysis are examined, it is seen that the period values change between 0.052 and 0.048 s for the first 4 modes. If the studies are examined, the mode shapes up to the first 5 modes gain importance in such structures [37]. The study also analyzed the number of modes up to ensure the effective mass of up to 95% participation condition in Turkey Seismic Code [30]. Since these period values remain in the same range with the elastic acceleration spectrum used in the study, the possibility of resonance of the structure under the effect of an earthquake should also be taken into consideration.

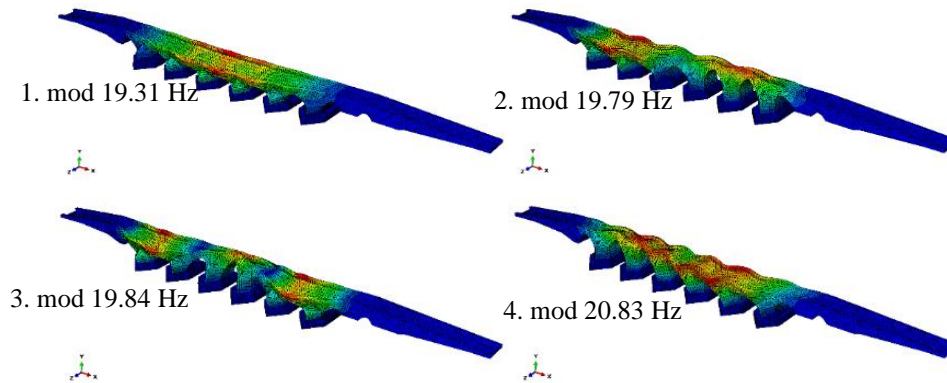


Figure 11. Free vibration modes and frequency values

5.1. Dynamic Analysis Results

As a result of the numerical analysis, it was found that the strength limits were not exceeded according to the stress distributions and damage profiles under constant stresses caused by the self-weight of the structure. The results of the nonlinear dynamic analysis in the time domain performed with 5 different scaled acceleration records were evaluated over the region of the structure that performs the maximum peak displacement and the DAMAGET crack distributions that represent the tensile damage defined in the material model. With the assessment, it has been observed that the acceleration record that causes the most unfavorable results for the building model is A2 (Bingöl) earthquake. For this reason, the damage profiles of the model were evaluated based on the A2 earthquake results.

According to this damage profile (Figure 12), the most critical tensile cracks occur both in the heel area and in the middle of the arch. Numerical analyzes by displacement provided detailed information on the seismic behavior of the structure for different acceleration records. In particular, nonlinear dynamic analysis provided evidence about damage distribution and the weakest elements. In Figure 12, the detailed results of the tensile damage on the bridge are given visually for A2 (Bingöl) earthquake recording. As can be seen in Fig. 13, in the analysis made for the Bingöl earthquake(A2), damage has occurred. In Figures 14 and 15, detailed views of the damage mechanisms for the damaged (A2) Bingöl earthquake are given.

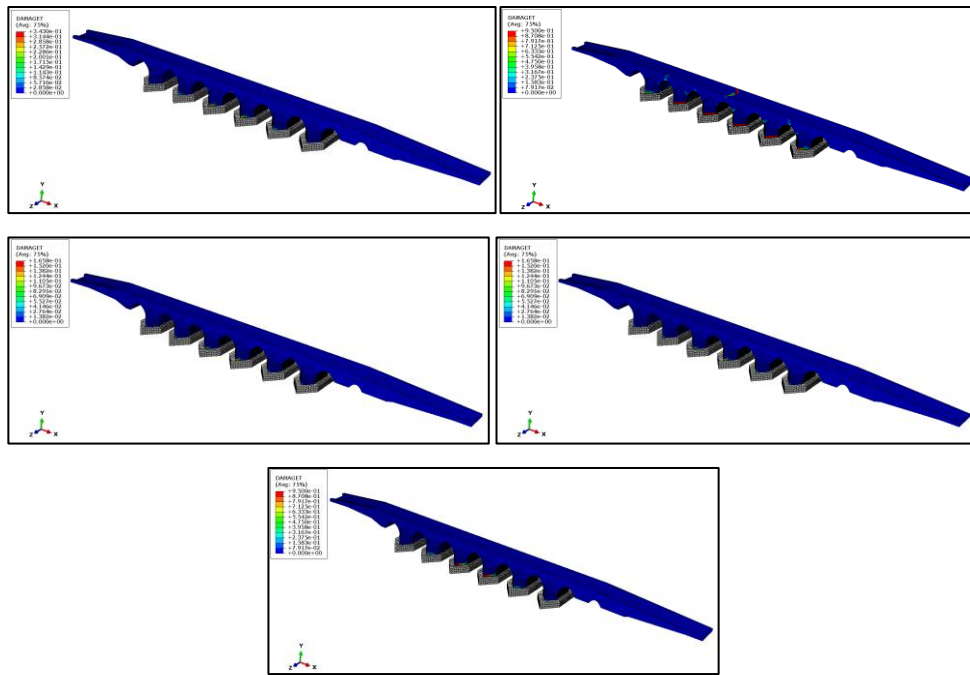


Figure 12. Dynamic analysis results

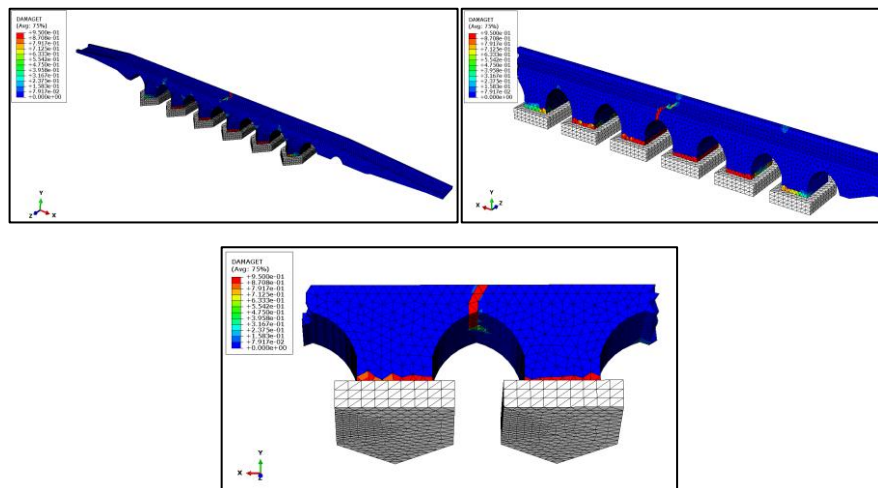


Figure 13. Damages on the bridge for A2 (Bingöl) earthquake

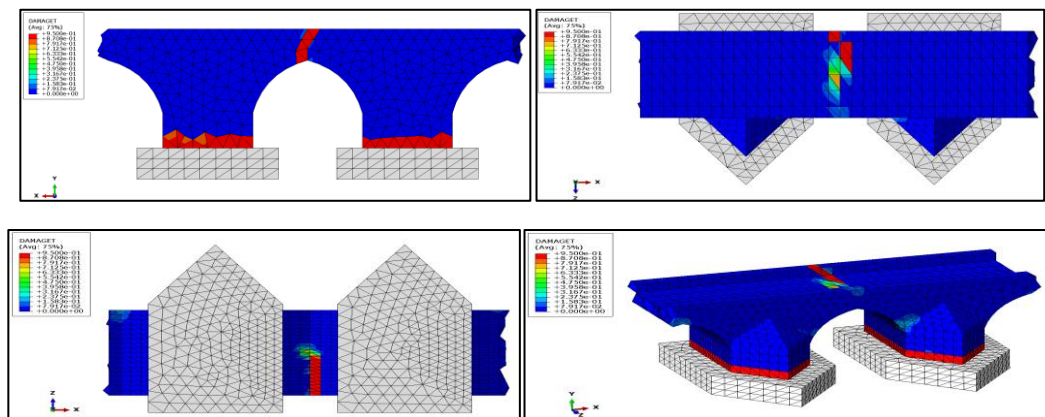


Figure 14. Damage profiles for A2 (Bingöl) earthquake

The maximum displacement point was selected for each analysis from the midpoint of the bridge where the crack occurred in A2 earthquake. According to the damage profile created using the Bingöl earthquake records, it was determined that the most critical tensile cracks occurred both in the heel area and in the middle of the bridge. Therefore, taking these data into consideration, the displacement time graphs in the model were obtained for the finite element number 1624 (Figure 15), which expresses the behavior at the point where the damage occurred for the A2 earthquake. In Figure 16, displacement-time graphs of the same finite element piece are given for each earthquake.

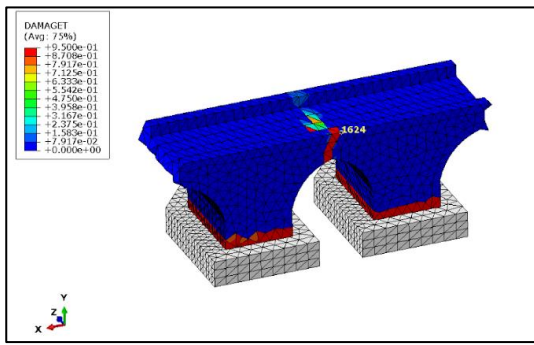


Figure 15. The nodal point considered for the displacement-time graphs (A2 Earthquake)

When we look at the displacement time graphs in Figure 16, a displacement of 0.012 m, 0.16 m, 0.8 m, 3 m and 0.2 m has occurred for the Historical Masonry Karaz bridge, Gölçük, Bingöl, Van, Erzincan and Elazığ earthquake records, respectively.

As we can see in Figures 13 and 14, in the Bingöl earthquake named as A2, damage occurred in the middle part of the bridge. When we look at Fig. 16, in the Erzincan earthquake we named as A4, although the maximum displacement of the node point in Fig. 15 was around 3m, damage occurred in the A2 Bingöl earthquake, where the maximum displacement was around 0.16 m. The most important reason for this is that the impact on the vertical component of the Bingöl earthquake is more destructive than other earthquakes. In addition, Bingöl earthquake can be said to be the best earthquake reflecting the real behavior, considering the location of the bridge.

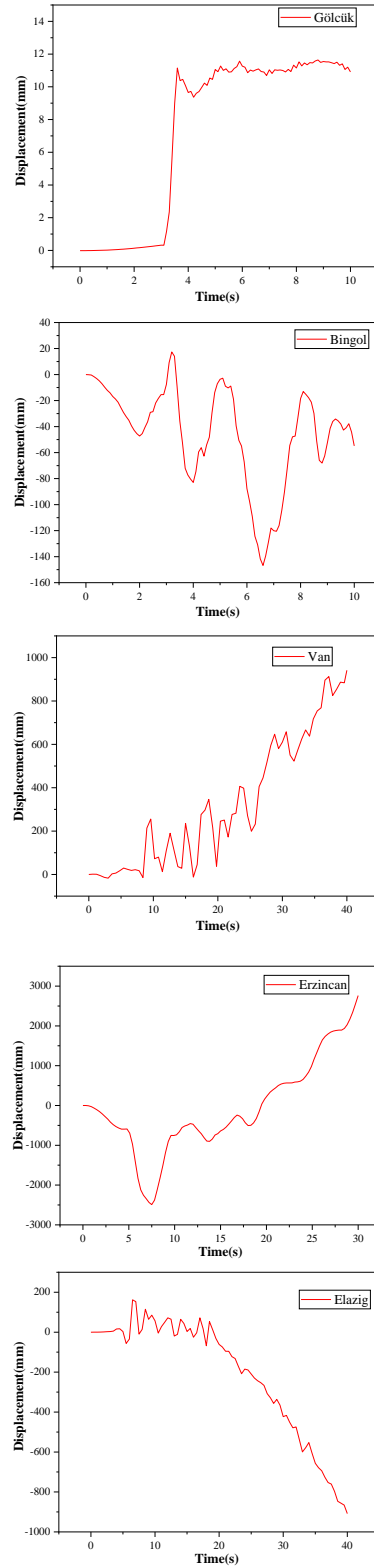


Figure 16. Displacement-time graphs

6. Conclusions

In this study, the three-dimensional finite element model of the Historical Karaz (Öznü) bridge, which has historical masonry and arch form, was created and the

behavior under the effect of earthquake was evaluated with the nonlinear analysis in the time history. The results of the nonlinear dynamic analysis in the time domain performed with 5 different scaled acceleration records were evaluated over the region of the structure that performs the maximum peak displacement and the crack distributions expressing the tensile damage defined in the material model. Detailed information on the seismic behavior of the structure is provided by numerical analysis by using different acceleration records for the displacement values at joint 1624 in the finite element model. In particular, nonlinear dynamic analysis provided evidence about damage distribution and the weakest elements. The following results can be proposed for the historical Karaz bridge, depending on the linear and nonlinear analysis findings obtained with the effect of the finite element behavior model:

- The three-dimensional finite element model of the masonry and arch shaped historical Karaz (Öznü) bridge was created and the behavior under the effect of an earthquake was examined using the nonlinear time history analysis and the damage status was evaluated.

- For this reason, the damage profiles of the model were evaluated based on the A2 earthquake results. According to this damage profile, the most critical tensile cracks occur both in the heel area and in the middle of the arch. The damage potential was found at a critical level in the middle parts of the bridge due to displacement. However, there was no displacement that would cause damage to the remaining parts of the bridge.

- Tensile stresses under earthquake load have reached the permissible tensile strength of masonry stones, especially on the upper sides of the middle belt, upper sides of the arch and the belt side road surface and pose a risk in terms of damage.

- When the periods of the bridge response spectrum obtained by time-history analysis and the natural vibration periods calculated by modal analysis are compared with the earthquake spectrum, the possibility of resonance on the bridge can be mentioned.

- Critical (large) relative displacement levels were not determined along the bridge height.

- Due to the modeling approach used, the behavior (damage, etc.) occurred in the regions where the stresses were concentrated in the elements. It should be noted that different modeling approaches may reveal different damage or collapse mechanisms due to other discontinuities that may exist in bridge elements. In future studies, field observation as well as analytical studies will contribute to the literature.

Conflict of Interest Statement

There is no conflict of interest between the authors.

Statement of Research and Publication Ethics

The study is complied with research and publication ethics

References

- [1] A. Özmen and E. Sayın, "Linear Dynamic Analysis of a Masonry Arch Bridge," in *International Conference on Innovative Engineering Applications*, 2018, no. September.
- [2] H. Güllü, "Investigation of Earthquake Effect of Historical Masonary Cendere Bridge," *Omer Halisdemir Univ. J. Eng. Sci.*, vol. 7, no. 1, pp. 245–259, 2018.
- [3] A. Ural, Ş. Oruç, A. Doğangün, and Ö. I. Tuluk, "Turkish Historical Arch Bridges and Their Deteriorations and Failures," *Eng. Fail. Anal.*, vol. 15, pp. 43–53, 2008.
- [4] Z. Celep and N. Kumbasar, *Betonarme Yapılar*. Istanbul: Beta, 2005.
- [5] B. Balun, Ö. F. Nemutlu, A. Benli, and A. Sari, "Estimation of probabilistic hazard for Bingol province, Turkey," *Earthq. Struct.*, vol. 18, no. 2, pp. 223–231, 2020.
- [6] A. Özmen and E. Sayın, "Seismic Assessment of a Historical Masonry Arch Bridge," *J. Struct. Eng. Appl. Mech.*, vol. 1, no. 2, pp. 95–104, 2018.
- [7] H. Güllü and H. S. Jaf, "Full 3D Nonlinear Time History Analysis of Dynamic Soil–Structure Interaction for a Historical Masonry Arch Bridge," *Environ. Earth Sci.*, vol. 75, no. 21, 2016.
- [8] M. Valente and G. Milani, "Damage Assessment and Collapse Investigation of Three Historical Masonry Palaces Under Seismic Actions," *Eng. Fail. Anal.*, vol. 98, pp. 10–37, 2019.

- [9] B. Sevim, A. Bayraktar, A. C. Altuniik, S. Atamtürktür, and F. Birinci, "Finite Element Model Calibration Effects on the Earthquake Response of Masonry Arch Bridges," *Finite Elem. Anal. Des.*, vol. 47, pp. 621–634, 2011.
- [10] A. Bayraktar, T. Türker, and A. C. Altunişik, "Experimental Frequencies and Damping Ratios for Historical Masonry Arch Bridges," *Constr. Build. Mater.*, vol. 75, pp. 234–241, 2015.
- [11] A. Bayraktar, A. C. Altunişik, F. Birinci, B. Sevim, and T. Türker, "Finite-Element Analysis and Vibration Testing of a Two-Span Masonry Arch Bridge," *J. Perform. Constr. Facil.*, vol. 24, no. 1, pp. 46–52, 2010.
- [12] M. Karaton, H. S. Aksoy, E. Sayın, and Y. Calayır, "Nonlinear Seismic Performance of a 12th Century Historical Masonry Bridge Under Different Earthquake Levels," *Eng. Fail. Anal.*, vol. 79, pp. 408–421, 2017.
- [13] E. Sayın, Y. Calayır, and M. Karaton, "Nonlinear Seismic Analysis of Historical Uzunok Bridge," in *Seventh National Conference on Earthquake Engineering*, 2021.
- [14] D. Proske and P. van Gelder, *Safety of Historical Stone Arch Bridges*. 2009.
- [15] G. Milani and P. B. Lourenço, "3D Non-linear Behavior of Masonry Arch Bridges," *Comput. Struct.*, vol. 110–111, pp. 133–150, 2012.
- [16] P. Lourenço and D. Oliveira, "Conservation of Ancient Constructions and Application to a Masonry Arch Bridge," in *Proceedings of the International Seminar on Theory and Practice in Conservations*, 2006.
- [17] L. Pelà, A. Aprile, and A. Benedetti, "Seismic assessment of masonry arch bridges," *Eng. Struct.*, vol. 31, pp. 1777–1788, 2009.
- [18] V. Sarhosis, S. De Santis, and G. de Felice, "A review of experimental investigations and assessment methods for masonry arch bridges," *Struct. Infrastruct. Eng.*, vol. 12, no. 11, pp. 1439–1464, 2016.
- [19] E. Işık, F. Avcil, E. Harirchian, E. Arkan, H. Bilgin, and H. B. Özmen, "Architectural Characteristics and Seismic Vulnerability Assessment of a Historical Masonry Minaret under Different Seismic Risks and Probabilities of Exceedance," *Buildings*, vol. 12, no. 8, 2022.
- [20] E. Işık, E. Harirchian, E. Arkan, F. Avcil, and M. Günay, "Structural Analysis of Five Historical Minarets in Bitlis (Turkey)," *Buildings*, vol. 12, no. 2, 2022.
- [21] M. Scamardo, M. Zucca, P. Crespi, N. Longarini, and S. Cattaneo, "Seismic Vulnerability Evaluation of a Historical Masonry Tower: Comparison between Different Approaches," *Appl. Sci.*, vol. 12, no. 21, 2022.
- [22] E. G. Çubuk, E. Sayın, A. Özmen, "Dynamic Analysis of Historical Masonry Arch Bridges under Different Earthquakes: The Case of Murat Bey Bridge," *Turkish J. Sci. Technol.*, vol. 17, no. 2, pp. 461–473, 2022.
- [23] F. Avcil, E. Işık, H. Bilgin, H. B. Özmen, "Sahaya Özgü Tasarım Spektrumlarının Anitsal Yığma Yapı Sismik Davranışın Etkisi," *Adıyaman Üniversitesi Mühendislik Bilim. Derg.*, vol. 16, pp. 165–177, 2022.
- [24] R. İzol, O. Türkmen, A. Gürel, and P. Turgut, "Mimar Sinan Camilerinde Sütunların Formları, Dikey ve Yanal Yük Kapasiteleri," *Bitlis Eren Üniversitesi Fen Bilim. Derg.*, pp. 649–659, 2022.
- [25] F. Avcil and E. Arkan, "Assessment of architectural heritage characteristics and seismic behavior of Ziyaeddin Han Tomb," *Bitlis Eren Univ. J. Sci. Technol.*, vol. 12, no. 2, pp. 79–85, 2022.
- [26] E. Işık, B. Antep, and İ. B. Karaşin, "Structural Analysis of Ahlat Emir Bayındır Bridge," *Bitlis Eren Univ. J. Sci. Technol.*, vol. 8, no. 1, pp. 11–18, 2018.
- [27] P. Zampieri, C. D. Tetougueni, and C. Pellegrino, "Nonlinear seismic analysis of masonry bridges under multiple geometric and material considerations: Application to an existing seven-span arch bridge," *Structures*, vol. 34, no. January, pp. 78–94, 2021.
- [28] H. Yalçın, L. Gülen, and M. Utkucu, "Active Fault Data Base and Assessment of Earthquake Hazard for Turkey and Surrounding Regions," *Earth Sci.*, vol. 34, no. 3, pp. 133–160, 2013.
- [29] "Ministry of Interior Disaster and Emergency Management Presidency," 2021. [Online]. Available: <https://en.afad.gov.tr/>.
- [30] TEC, Turkish Earthquake Code. Ankara, Turkey, 2018.
- [31] "SeismoMatch Software." 2020.
- [32] American Society of Civil Engineers, *Minimum Design Loads and Associated Criteria for Buildings and Other Structures*. 2017.
- [33] O. C. Zienkiewicz and R. L. Taylor, *The Finite Element Method*. Butterworth-Heinemann, 2006.

- [34] J. Campbell and M. Durán, “Numerical model for nonlinear analysis of masonry walls,” *Rev. la Constr.*, vol. 16, no. 2, pp. 189–201, 2017.
- [35] J. Lee and G. L. Fenves, “Plastic-Damage Model for Cyclic Loading of Concrete Structures,” *J. Eng. Mech.*, vol. 124, no. 8, pp. 892–900, 1998.
- [36] J. Lubliner, J. Oliver, S. Oller, and E. Onate, “A Plastic Damage Model for Concrete,” *Int. J. Solids Struct.*, vol. 25, no. 3, pp. 299–326, 1989.
- [37] N. Bayülke, Depremlerde Hasar Gören Yapıların Onarım ve Güçlendirilmesi. İzmir: İnşaat Mühendisleri Odası İzmir Şubesi, 2010.